An Algorithm for No-Reference Image Quality Assessment Based on Log-Derivative Statistics of Natural Scenes

Yi Zhang and Damon M. Chandler

laboratory of Computational Perception and Image Quality
School of Electrical and Computer Engineering
Oklahoma State University

ABSTRACT

In this paper, we propose a new method for blind/no-reference image quality assessment based on the log-derivative statistics of natural scenes. The new method, called DErivative Statistics-based Image QUality Evaluator (DESIQUE), extracts image quality-related statistical features at two image scales in both the spatial and frequency domains, upon which a two-stage framework is employed to evaluate image quality. In the spatial domain, normalized luminance values of an image are modeled in two ways: point-wise based statistics for single pixel values and pairwise-based log-derivative statistics for the relationship of pixel pairs. In the frequency domain, log-Gabor filters are used to extract the high frequency component of an image, which is also modeled by the log-derivative statistics. All of these statistics are characterized by a generalized Gaussian distribution model, the parameters of which form the underlying features of the proposed method. Experiment results show that DESIQUE not only leads to considerable performance improvements, but also maintains high computational efficiency.

Keywords: Image quality assessment, derivative statistics, generalized Gaussian distribution, log-Gabor filer

1. INTRODUCTION

In recent years, image quality assessment (IQA) has become an important issue in many fields and applications such as image acquisition, transmission, compression, restoration and enhancement. As the ultimate consumers, humans can easily give subjective scores to measure the qualities of images they observe. However, it is a challenging work to embed such a mechanism into an image processing system whose goal is to maximize visual quality at a given cost. Therefore, an automatic quality measurement method that can give scores to images in a meaningful agreement with subjective judgment of human being is needed.

While full-reference (FR) and reduced-reference (RR) IQA algorithms provide a useful and effective way to evaluate quality of distorted images, in many cases however, the reference image or even the partial information of images are unknown, in which case a no-reference (NR) IQA algorithm is desired. NR IQA algorithms can be further classified into distortion-specific and non-distortion-specific, based on the prior knowledge of the distortion type. Most existing NR IQA methods are distortion-specific, assuming that the distortion type is known, such as the white noise and blurring (e.g., Refs. 1–4), JPEG/JPEG2000 (e.g., Refs. 5–16). This underlying assumption limits the application domain of these algorithms. Non-distortion-specific algorithms do not consider the prior knowledge of distortion type, but instead they give quality scores assuming that image to be evaluated has a same distortion type as those in the training database. These methods usually involve machine learning techniques, where distinct features related to image quality are extracted to train learning models and then these models are used to evaluate the quality of testing images.

In this paper, we propose a non-distortion-specific IQA method, called DErivative Statistics-based Image QUality Evaluator (DESIQUE), which extracts log-derivative statistics of natural images in both the spatial and frequency domain. In the spatial domain, normalized luminance coefficients are modeled in two ways: (1) point-wise based statistics for single pixel values (following Ref. 17), and (2) pairwise-based log-derivative statistics for the relationship of pixel pairs. In the frequency domain, log-derivative statistics are applied to the magnitudes of log-Gabor filter band coefficients to characterize the distribution of the high spatial frequencies at two orientations (horizontal and vertical). All the statistics extracted can be characterized by a generalized

Image Quality and System Performance X, edited by Peter D. Burns, Sophie Triantaphillidou,
Proc. of SPIE-IS&T Electronic Imaging, SPIE Vol. 8653, 86530J • © 2013 SPIE-IS&T
CCC code: 0277-786X/13/$18 • doi: 10.1117/12.2001342

Gaussian distribution (GGD) model which has been used before to model the subband statistics of natural images in IQA.[18,19] The DESIQUE analyzes images over two scales and captures 64 features in total (32 features for each scale) to predict the image quality using the two-stage framework from Refs. 17 and 19. We show that the proposed method correlates highly with human subjective assessment of image qualities on many databases.

This paper is organized as follows. In Section 2 we review the previous work in non-distortion-specific NR IQA algorithms. In Section 3 we provide detailed descriptions on how the log-derivative statistics based features are extracted, upon which image quality is evaluated. We present experiment results on different image database and evaluate the performance of different algorithms in Section 4 and finally give conclusions of the paper in Section 5.

2. PREVIOUS WORK

Most present-day NR IQA algorithms are distortion-specific which assume that the distortion type is known, and only determine severity. In comparison, the non-distortion-specific NR IQA algorithms are more useful in practice, however more difficult to develop, resulting in fewer researchers working in this area. These algorithms often assume that examples with the same or similar distortion types are available, and thus by mapping the test image with example ones in the feature space, the distortion types as well as the qualities of the test images can be assessed. The non-distortion-specific NR IQA approaches usually follow one of the following two trends: (1) training/learning based approach and (2) natural scene statistics (NSS) based approach.

2.1 Training/Learning Based NR IQA Method

Training/learning-based NR IQA approaches often rely on a large number of features that are designed to capture relevant factors that affect image quality. Then different regression techniques such as support vector machine (SVM) and neural network are employed to learn the mapping from feature space to image quality. For example, Tong *et al.*[20] proposed to learn from the training examples which contain both the high and low quality classes. Then a binary classifier is built, upon which quality of an un-labeled image is denoted by the extent to which it belongs to these two classes. Tang *et al.*[21] proposed a learning-based blind image quality (LBIQ) measure that combines and incorporates numerous low-level image quality features stemming from natural image measures and texture statistics with a regression algorithm, which is able to correlate the underlying structure of distorted images with perceptual image quality without need of a reference image. Li *et al.*[22] developed a general regression neural network (GRNN) based NR method, which assess image quality by approximating a function relationship between features and subjective mean opinion scores using GRNN. Ye and Doermann[23,24] proposed a block based NR IQA method which uses a visual codebook for feature space quantization. Then image quality is evaluated by learning mappings from the quantization feature space to image quality scores using either example-based method or support vector machine.

2.2 NSS Based NR IQA Method

NSS-based NR IQA approaches usually contain two stages which require some training: (1) distortion identification followed by (2) distortion-specific quality assessment. Once trained, the framework does not require any knowledge of the distortion and the framework is modular in that it can be extended to any number of distortions. Different NSS-based NR algorithms often have different features extracted and different training methods applied. The most state-of-art NSS-based NR algorithms are: (1) BIQI;[25] (2) BLIINDS-II;[26] (3) DIIVINE[19] and (4) BRISQUE.[17]

BIQI, the blind image quality index, is a wavelet-based NR IQA method which extracts image features by modeling the wavelet subband coefficients based on GGD. It operates on wavelet transform with three scales and three orientations using Daubechies 9/7 wavelet basis, and a number of 18 features are extracted for each image. DIIVINE improves upon BIQI by using a steerable pyramid wavelet transform with two scales and six orientations, and a total number of 88 features are extracted based on the statistical properties of the multi-scale, multi-orientation wavelet subbands. BLIINDS-II measures image quality based on the discrete cosine transform (DCT) coefficients of image patches. It derives a generalized NSS-based model for local DCT coefficients and transforms the model parameters into features used for perceptual image quality score prediction, which correlates highly with human subjective judgment.

BRISQUE is another NSS-based NR IQA method which operates in the spatial domain. The underlying features used derive from the empirical distribution of locally normalized luminance and products of locally normalized luminance under a spatial NSS model. No transform (e.g., DCT, wavelet, etc) is required, distinguishing it from previous NR IQA approaches. It operates on two image scales and for each scale, 18 features are extracted. Despite its simplicity, this algorithm has shown a much higher performance than the previous ones and even challenges FR IQA methods. It also has a very low computational complexity, making it well suited for real time applications. So far, it is the best-performing NSS-based NR IQA methods developed.

3. ALGORITHM

The proposed DESIQUE algorithm is based on the assumption that some derivative-based statistical properties of natural images in both the spatial and frequency domains will vary significantly in the presence of distortions, rendering them *un-natural*, and that by characterizing this un-naturalness, image quality can be evaluated. DESIQUE employs the same two-stage framework used in DIIVINE and BRISQUE: (1) distortion identification followed by (2) distortion-specific quality assessment, and extracts log-derivative based statistic features in the spatial and frequency domains using five derivative types. Finally, these features are used by the aforementioned two-stage framework to estimate image quality. In this section, we will provide details for each steps.

3.1 Log-Derivative Statistics

Derivative statistics of natural images were first studied in Ref. 27, in which difference of gray level values in digital images between one pixel and its neighboring pixels was considered as its derivatives. Motivated by the work in Refs. 17 and 28, derivatives between pairs of pixels can have five orientations: horizontal, vertical, main-diagonal and secondary-diagonal, and combined-diagonal.

Here, to efficiently model natural images/image subbands by using the distribution of derivative statistics, we first compute the logarithm of each pixel value to create new images/image subbands J by

$$J(i,j) = log[I(i,j) + K] \tag{1}$$

where K is a small constant that prevents $I(i,j)$ to be zero. Then, we compute the five types of log-derivatives:

$$D1 : \nabla_x J(i,j) = J(i,j+1) - J(i,j) \tag{2}$$
$$D2 : \nabla_y J(i,j) = J(i+1,j) - J(i,j) \tag{3}$$
$$D3 : \nabla_{xy} J(i,j) = J(i+1,j+1) - J(i,j) \tag{4}$$
$$D4 : \nabla_{yx} J(i,j) = J(i+1,j-1) - J(i,j) \tag{5}$$
$$D5 : \nabla_x \nabla_y J(i,j) = J(i,j) + J(i+1,j+1) - J(i,j+1) - J(i+1,j) \tag{6}$$

In the following sections, we will show that histogram distributions of these five types of log-derivative statistics are effective in modeling natural images — their profiles change significantly in the presence of different distortions, and these changes are used to estimate quality.

3.2 Log-Derivative Statistics Based Features

As mentioned in Section 2, recent work has focused on modeling natural scene statistics either in the spatial domain[17] or in a transform domain (e.g., Gabor filters, DCT, wavelets) (see Refs. 19, 25 and 26). However, the perceptual quality can be influenced by both the spatial and frequency information in an image. Thus, the proposed DESIQUE features will consist of two parts: (1) the spatial domain features and (2) the frequency domain features. Figure 1 shows a block diagram illustrating how to extract DESIQUE features in both domains.

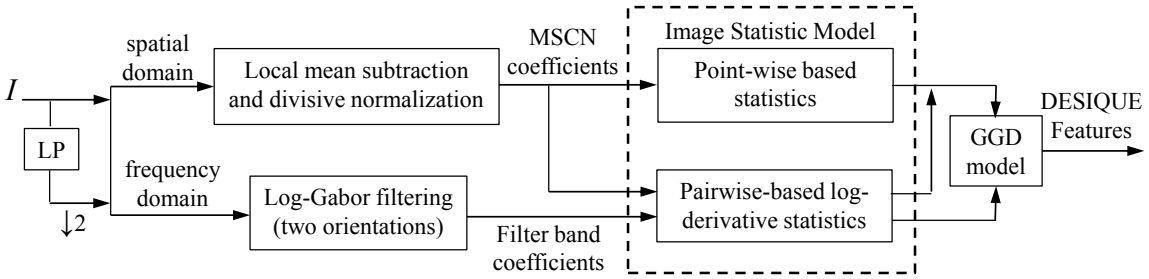

Figure 1. A block diagram on DESIQUE feature extraction. Note that the filter band coefficients will only contain the first scale of the log-Gabor filter subbands corresponding to the high frequency components of an image. LP means low-pass filter.

3.2.1 Modeling image statistics in the spatial domain

The features extracted in the spatial domain consists of two types: (1) point-wise based statistics for single pixel values (same as Ref. 17) and (2) pairwise-based log-derivative statistics for the relationship of pixel pairs. Specifically, given an image $I(i,j)$, we first compute locally normalized luminance via local mean subtraction and divisive normalization[29] defined as:

$$\hat{I} = \frac{I(i,j) - \mu(i,j)}{\sigma(i,j) + C}, \tag{7}$$

where $i \in 1, 2, \cdots, M$, $j \in 1, 2, \cdots, N$ are spatial indices; M, N are the image height and width respectively; $C = 1$ is a constant that prevents the denominator to be zero. The quantities $\mu(i,j)$ and $\sigma(i,j)$ are defined as

$$\mu(i,j) = \sum_{k=-K}^{K} \sum_{l=-L}^{L} \omega_{k,l} I_{k,l}(i,j), \tag{8}$$

$$\sigma(i,j) = \sqrt{\sum_{k=-K}^{K} \sum_{l=-L}^{L} \omega_{k,l} (I_{k,l}(i,j) - \mu(i,j))}, \tag{9}$$

where $\omega = \{\omega_{k,l} | k = -K, \cdots, K, l = -L, \cdots, L\}$ is a 2D circularly-symmetric Gaussian weighting function sampled out to three standard deviations and rescaled to unit volume. As in Ref. 17, we also define $K = L = 3$.

According to Ref. 17, the mean-subtracted contrast-normalized (MSCN) coefficients $\hat{I}(i,j)$ can be modeled by a zero-mean GGD given by:

$$f(x; \alpha, \sigma^2) = \frac{\alpha}{2\beta\gamma(1/\alpha)} exp(-|x|/\beta)^{\alpha} \tag{10}$$

where $\beta = \sigma\sqrt{\frac{\gamma(1/\alpha)}{\gamma(3/\alpha)}}$ and $\gamma(x) = \int_0^{\infty} t^{x-1} e^{-t} dt (x > 0)$ is the gamma function. The parameter α controls the 'shape' of the distribution and σ^2 controls the variance. We estimate the two-parameter GGD model using the moment-matching based approach proposed in Ref. 30 and these two values form the first set of features in the spatial domain that will be used to capture image distortion by DESIQUE.

The other set of features we extract in the spatial domain are formed by modeling the relationship of neighboring MSCN coefficient pairs based on log-derivative statistics. We model the relationship between two adjacent MSCN coefficients by using the five types of log-derivatives previously defined by Eqs. (2)-(6). Here $J(i,j) = ln(|\hat{I}(i,j)| + K)$ and $K = 0.1$ is a constant that prevents $\hat{I}(i,j)$ to be zero. Under the Gaussian coefficient model, and assuming the MSCN coefficients are zero mean and unit variance, these log-derivative values also obey the generalized Gaussian distribution and thus their parameters (α, σ^2) can be estimated by using the method proposed in Ref. 30. These ten parameters form the second part of DESIQUE features extracted in the spatial domain.

Figure 2. Reference image *sailing2* and its five distorted versions in the LIVE database.[31] *From left to right*: reference image, Gaussian blur, fast-fading, JPEG2000 compression, JPEG compression and Gaussian white noise.

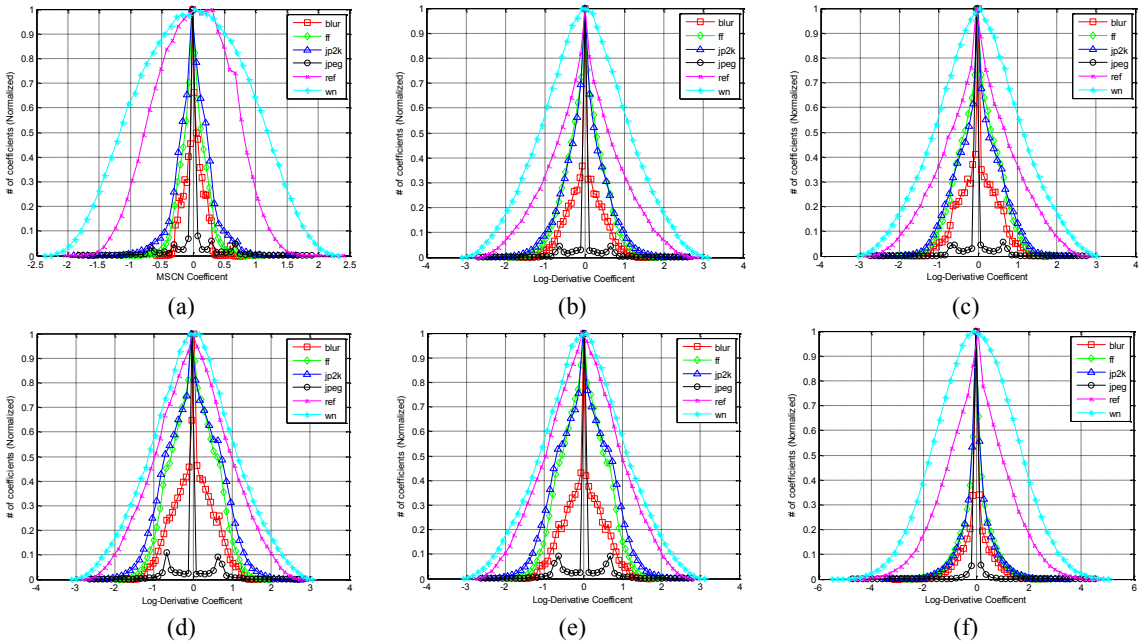

Figure 3. Histogram of MSCN coefficients (a) and their five types of log-derivatives statistics (b-f) for each of the five distorted versions of image *sailing2* (shown in Figure 2). Distortions from the LIVE database - JPEG2000 (jp2k) and JPEG compression (jpeg), Additive white noise (wn), Gaussian blur (blur), and a Rayleigh fast-fading channel simulation (ff). Notice that the distortions tend to affect the peakness of the characteristic profile observed for the reference images.

In order to visualize how the aforementioned two statistics of the MSCN coefficients in the spatial domain vary as a function of distortions, Figure 2 shows one reference image and its five distorted versions from the LIVE database,[31] and Figure 3 plots their corresponding histograms of MSCN coefficients. Notice that both the point-wise-based statistics and the pairwise-based log-derivative statistics of MSCN coefficients in the spatial domain change significantly in the presence of different distortions, allowing them to produce efficient features for evaluating image quality.

3.2.2 Modeling image statistics in the frequency domain

To estimate quality based on frequency-domain statistics, we decompose an image using log-Gabor filter on two orientations (horizontal and vertical) and use the first layer of the image subband (corresponding to the high spatial frequency) for analysis. Again we apply the five types of log-derivatives previoiusly defined by Eqs. (2)-(6). Here $J(i,j) = ln(|g(i,j)| + K)$, $|g(i,j)|$ is the magnitude of the log-Gabor filter subband coefficient and $K = 0.1$ is a constant that prevents $g(i,j)$ to be zero. Again the coefficients' log-derivative statistics for each of these

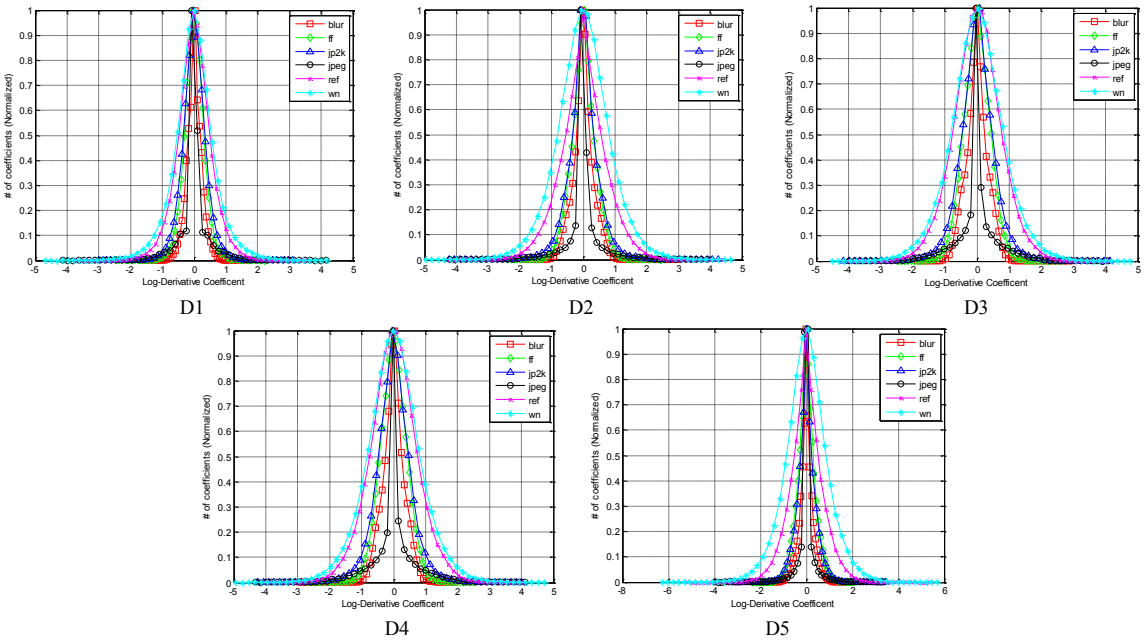

Figure 4. Histograms of the log-derivative statistics of the filter subband coefficients for one reference image (Image *sailing2*) and its five distorted versions (shown in Figure 2). D1-D5 correspond to the five log-derivative types defined by Eqs. (2)-(6). Distortions from the LIVE database - JPEG2000 (jp2k) and JPEG compression (jpeg), Additive white noise (wn), Gaussian blur (blur), and a Rayleigh fast-fading channel simulation (ff). Notice that the histogram profile vary significantly in peakness when distortions are presented.

subbands obey the generalized Gaussian distribution. The parameters (α, σ^2) estimated yield 20 DESIQUE features (2 subbands $\times$ 5 derivative types $\times$ 2 parameters/derivative type) extracted in the frequency domain.

To illustrate how the log-derivative statistics of the filter subband coefficients behave as a function of distortions in the frequency domain, Figure 4 plots their corresponding histograms for a reference image and its five distorted versions (shown in Figure 2) on horizontal orientation (similar results can also be obtained on vertical orientation). Notice that the log-derivative statistics of the subband coefficient change profiles significantly in the presence of different distortions, making them effective features for identifying distortions and measuring image quality.

Since images are naturally multi-scale and distortions affect image structure across scales, following from Ref. 17, we extract all spatial and frequency features at two scales: the original image scale and a low pass filtered and down-sampled (by a factor of 2) scale. Thus a total of 64 features (32 at each scale) are used to identify distortions and to perform distortion-specific quality assessment.

3.3 Quality Evaluation

Given the 64 features, DESIQUE employs the same two-stage framework used in DIIVINE and BRISQUE: (1) distortion identification and (2) distortion-specific quality assessment. For the distortion identification stage, a trained support vector classification (SVC) machine is employed to measure the probability that the distortion in the distorted images falls into one of the n distortion classes, denoted by $\vec{p}$, an n-dimensional vector of probabilities. For the distortion-specific quality assessment stage, support vector regression (SVR) machine with n trained regression models are employed to map the feature vectors to an associated quality score, denoted by $\vec{q}$, an n-dimensional vector of estimated qualities obtained from these n trained regression models. Then the final estimate quality is computed as $\vec{p} \cdot \vec{q}$.

4. RESULTS

In this section, the performance of DESIQUE is analyzed in terms of its ability to predict subject ratings of image quality. To assess its predictive performance, three databases of subjective image quality were used: 1. the LIVE database[31] (used for training), 2. the CSIQ database,[32] and 3. the TID database.[33]

4.1 Training

Once we have these 64 features, a two-stage framework is trained on LIVE[31] to measure image quality. First, a classification model is trained by a Support Vector Classification (SVC) Machine to measure the probability that each distortion type exist in certain distorted images. Second, for each distortion type, a particular regression model is trained by the Support Vector Regression (SVR) Machine that will map certain feature vector to the associated quality score. Like DIIVINE, the classifier does not produce a hard classification, but instead giving the probability that the input belongs to each classes. Finally, each distortion-specific quality scores are weighted by the probability of that distortion type presenting in the image to give the final quality score.

4.2 Testing

In order to evaluate the performance of our proposed method, we use the CSIQ and TID databases for testing. We applied a four-parameter logistic transform to bring predict values on the same scales as the DMOS/MOS values.

The performance measures used are Spearman rank-order correlation coefficient (SROCC), Pearson linear correlation coefficient (CC) and root mean square error (RMSE). A value close to 1 for SROCC and CC and 0 for RMSE indicate good performance in terms of correlation with human opinion. We compared DESIQUE with various FR and NR quality assessment methods for which code is publicly available. The five FR methods were PSNR,[34] SSIM,[35] MS-SSIM,[36] VIF,[37] and MAD.[38] The three NR methods were DIIVINE,[19] BLIINDS-II,[26] and BRISQUE,[17] all of which are NSS-based and trained on LIVE.

4.3 Overall Performance

Table 1 shows the performance of DESIQUE and other quality assessment algorithms on the entire set of images from CSIQ and TID. Also shown in Table 1 are the average performance across database for CC, SROCC and RMSE. Notice that all these FR IQA algorithms compared are only applied on those four distortion types that have been trained. The highlighted entries represent the best performance in the database for the particular database for FR/NR IQA.

Table 1. Overall performances of DESIQUE and other algorithms. Italicized entries denote NR algorithms. Results of the best-performing FR algorithm are bolded, and results of the best-performing NR algorithm are italicized and bolded.

		PSNR	SSIM	MS-SSIM	VIF	MAD	*DIIVINE*	*BLIINDS-II*	*BRISQUE*	*DESIQUE*
CC	CSIQ	0.9075	0.8510	0.9497	0.9670	**0.9738**	*0.8544*	*0.9006*	*0.9235*	***0.9338***
	TID	0.8476	0.7358	0.9117	**0.9499**	0.9469	*0.8774*	*0.8638*	*0.9066*	***0.9165***
	Average	0.8841	0.8060	0.9349	0.9603	**0.9633**	*0.8634*	*0.8862*	*0.9169*	***0.9270***
SROCC	CSIQ	0.9217	0.8763	0.9528	0.9587	**0.9671**	*0.8284*	*0.8726*	*0.9002*	***0.9179***
	TID	0.8703	0.7674	0.8966	**0.9399**	0.9352	*0.8910*	*0.8396*	*0.8975*	***0.9129***
	Average	0.9016	0.8338	0.9309	0.9514	**0.9547**	*0.8528*	*0.8597*	*0.8991*	***0.9159***
RMSE	CSIQ	0.1187	0.1484	0.0885	0.0720	**0.0643**	*0.1468*	*0.1228*	*0.1084*	***0.1011***
	TID	0.8400	1.0722	0.6504	**0.4951**	0.5091	*0.7597*	*0.7977*	*0.6681*	***0.6335***
	Average	0.4002	0.5089	0.3078	0.2371	**0.2379**	*0.3860*	*0.3862*	*0.3268*	***0.3089***

From Table 1 it is clear that compared with other NR IQA methods, DESIQUE performs quite well in correlation with human perception. It improves upon BRISQUE and is superior to DIIVINE and BLIINDS-II. Further, it even challenges some of the FR IQA methods like PSNR and SSIM. The last rows of the results in

Table 1 show the average SROCC, CC and RMSE, where the averages are weighted by the number of distorted images tested in each database. On an average, DESIQUE demonstrates the best NR IQA performance. In summary, when looking at the overall performance across database, the proposed DESIQUE has a better average performance than other NR IQA methods.

4.4 Computational Analysis

Having demonstrated that DESIQUE performs well in predicting image quality, now we also show that it has a low computational complexity. Although DESIQUE extracts features in both the spatial and frequency domains to evaluate image quality and the number of features (64) is larger than that of BRISQUE (which only has 36 features), it is still quite efficient in computation. To demonstrate, we compared the overall computation time of DESIQUE with three NR IQA methods (BLIINDS-II, DIIVINE and BRISQUE) on different image size (256×256, 512×512, 1024×1024, and 1600×1600 pixels). The test was performed on a modern desktop computer (AMD Phenom II ×4 965 Processor at 3.39 GHz, 4.00 GB RAM, Windows 7 Pro 64-bit, Matlab 7.8.0). Table 2 shows the average runtime of each algorithm in seconds, where the average is taken over 100 trials. Compared with other NR IQA algorithms, DESIQUE is not only of higher-performance, but also maintains a significant computational efficiency.

Table 2. Runtime requirements (seconds/image) for four NR IQA methods on different image sizes.

	256×256	512×512	1024×1024	1600×1600
BRISQUE	0.167	0.265	0.666	1.431
DESIQUE	0.178	0.479	1.679	3.935
DIIVINE	9.322	24.800	93.176	254.585
BLIINDS-II	23.956	95.242	377.364	>1060

5. CONCLUSION

This paper presented a new algorithm for no-reference image quality assessment (DESIQUE), which operates by using log-derivative statistics of natural scenes. DESIQUE extracts log-derivative-based statistical features at two image scales in both the spatial and frequency domains, upon which a two-stage framework is employed to evaluate quality. We demonstrated that DESIQUE can achieve better performance in predicting image quality than many other well-known NR IQA methods across various databases. We also showed that DESIQUE is computationally efficient.

ACKNOWLEDGMENTS

This material is based upon work supported by the National Science Foundation Awards 0917014 and 1054612, and by the U.S. Army Research Laboratory (USARL) and the U.S. Army Research Office (USARO) under contract/grant number W911NF-10-1-0015.

REFERENCES

[1] Li, X., "Blind image quality assessment," in [*Proc. of Image Processing (ICIP2002), IEEE International Conference*], **1**, 1449–1452 (2002).

[2] Gabarda, S. and Cristobal, G., "No-reference image quality assessment through von mises distribution," *Journal of the Optical Society of America A (JOSA A)* **29**, 2058–2066 (2012).

[3] Brandao, T. and Queluz, M. P., "No-reference image quality assessment based on DCT domain statistics," *Signal Processing* **88**, 822–833 (2008).

[4] Cohen, E. and Yitzhaky, Y., "No-reference assessment of blur and noise impacts on image quality," *Signal, Image and Video Processing* **4**(3), 289–302 (2010).

[5] Wang, Z., Bovik, A. C., and Evans, B. L., "Blind measurement of blocking artifacts in images," in [*Proc. IEEE Int. Conf. Image Proc*], **3**, 981–984 (September 2000).

[6] Bovik, A. C. and Liu, S., "DCT-domain blind measurement of blocking artifacts in DCT-coded images," in [*Proc. IEEE Int. Acoust., Speech and Signal Processing*], **3**, 1725–1728 (May 2001).

[7] Wang, Z., Sheikh, H. R., and Bovik, A. C., "No-reference perceptual quality assessment of JPEG compressed images," in [*Proc. of IEEE Int. Conf. on Image Processing*], **1**, 477–480 (2002).

[8] Pan, F., Liu, X., Rahardja, S., Ong, E. P., and Lin, W. S., "Measuring blocking artifacts using edge direction information," in [*2004 IEEE International Conference on Multimedia and Expo (ICME)*], **2**, 1491–1494 (June 2004).

[9] Perra, C., Massidda, F., and Giusto, D. D., "Image blockiness evaluation based on sobel operator," in [*International Conference on Image Processing*], (2005).

[10] Sheikh, H. R., Bovik, A. C., and Cormack, L., "No-reference quality assessment using natural scene statistics: JPEG2000," *IEEE Trans. Image Processing* **14**, 1918–1927 (November 2005).

[11] Zhou, J., Xiao, B., and Li, Q., "A no reference image quality assessment method for JPEG2000," in [*IEEE International Conference on Neural Networks*], 863–868 (June 2008).

[12] Li, M., Zhang, H., and Zhang, C., "No-reference quality assessment for JPEG2000 compressed images," in [*International Conference on Image Processing (ICIP)*], 3539–3542 (2004).

[13] Park, C.-S., Kim, J.-H., and Ko, S.-J., "Fast blind measurement of blocking artifacts in both pixel and DCT domains," *Journal of Mathematical image and vision* **28**(3), 279–284 (2007).

[14] Suresh, S., Babu, R. V., and Kim, H. J., "No-reference image quality assessment using modified extreme learning machine classifier.," *Appl. Soft Comput.* **9**(2), 541–552 (2009).

[15] S.Suthaharan, "No-reference visually significant blocking artifact metric for natural scene images," *Signal Processing* **89**(8), 1647–1652 (2009).

[16] Zhang, J., Ong, S. H., and Le, T. M., "Kurtosis-based no-reference quality assessment for JPEG2000 images," *Signal Processing: Image Communication* **26**, 13–23 (January 2011).

[17] Mittal, A., Moorthy, A. K., and Bovik, A. C., "No-reference image quality assessment in the spatial domain," *IEEE Transations on Image Processing* (2012 (to appear)).

[18] Li, Q. and Wang, Z., "Reduced-reference image quality assessment using divisive normalization-based image representation," *IEEE Journal of Selected Topics in Signal Processing* **3**, 202–211 (April 2009).

[19] Moorthy, A. K. and Bovik, A. C., "Blind image quality assessment: From natural scene statistics to perceptual quality.," *IEEE Transactions on Image Processing* **20**(12), 3350–3364 (2011).

[20] Tong, H., Li, M., Zhang, H., and Zhang, C., "Learning no-reference quality metric by examples," in [*Proc. 11th Int. Multimedia Modelling Conf.*], (January 2005).

[21] Tang, H., Joshi, N., and Kapoor, A., "Learning a blind measure of perceptual image quality," in [*International Conference on Computer Vision and Pattern Recognition*], (2011).

[22] Li, C., Bovik, A. C., and Wu, X., "Blind image quality assessment using a general regression neural network," *IEEE Transaction on Neural Networks* **22**, 793–799 (May 2011).

[23] Ye, P. and Doermann, D., "No-reference image quality assessment using visual codebook," in [*International Conference on Image Processing*], (2011).

[24] Ye, P. and Doermann, D., "No-reference image quality assessment using visual codebook," *IEEE Transaction on Image Processing* **21**, 3129–3138 (July 2012).

[25] Moorthy, A. K. and Bovik, A. C., "A two-step framework for constructing blind image quality indices," *IEEE Signal Processing Letters* **17**, 513–516 (May 2010).

[26] Saad, M. A. and Bovik, A. C., "Blind image quality assessment: A natural scene statistics approach in the DCT domain," *IEEE Transactions on Image Processing* **21**, 3339–3352 (2012).

[27] Huang, J. and Murnford, D., "Statistics of natural images and models," in [*IEEE Computer Society Conference on Computer Vision and Pattern Recognition*], (1999).

[28] Chen, T.-L., "On the statistics of natural images," *Phd Thesis, Division of Applied Mathematics at Brown University* (May 2005).

[29] Ruderman, D. L., "The statistics of natural images," *Network computation in neural systems* **5**(4), 517–548 (1994).

[30] Sharifi, K. and Leon-Garcia, A., "Estimation of shape parameter for generalized gaussian distribution in subband decompositions of video," *IEEE Transactions on Circuits and System for Video Technology* **5**(1), 52–56 (1995).

[31] Sheikh, H. R., Wang, Z., Bovik, A. C., and Cormack, L. K., "Image and video quality assessment research at LIVE." Online. http://live.ece.utexas.edu/research/quality/.

[32] University, C. P. . I. Q. L. O. S., "CSIQ image database," (2009). http://vision.okstate.edu/csiq/.

[33] Ponomarenko, N., Lukin, V., Zelensky, A., Egiazarian, K., Carli, M., and Battisti, F., "TID2008 - a database for evaluation of full-reference visual quality assessment metrics," *Advances of Modern Radioelectronics* **10**, 30–45 (2009).

[34] T1.TR.74-2001, A., *Objective Video Quality Measurement Using a Peak-Signal-to-Noise-Ratio (PSNR) Full Reference Technique* (2001).

[35] Wang, Z., Bovik, A. C., Sheikh, H. R., and Simoncelli, E. P., "Image quality assessment: From error visibility to structural similarity," *IEEE Trans. Image Process.* **13**, 600–612 (April 2004).

[36] Wang, Z., Simoncelli, E. P., and Bovik, A. C., "Multiscale structural similarity for image quality assessment," in [*Conference Record of the Thirty-Seventh Asilomar Conference on Signals, Systems and Computers*], **2**, 1398 – 1402 Vol.2 (Nov 2003).

[37] Sheikh, H. R. and Bovik, A. C., "Image information and visual quality," *IEEE Transactions on Image Processing* **15**(2), 430–444 (2006).

[38] Larson, E. C. and Chandler, D. M., "Most apparent distortion: full-reference image quality assessment and the role of strategy," *Journal of Electronic Imaging* **19**(1), 011006 (2010).